Lecture Notes on Scale-Model Experiments

Nielsen, Peter Vilhelm

Publication date:
1999

Document Version
Publisher's PDF, also known as Version of record

Aalborg **UNIVERSITY**

Lecture N

Lecture Notes on Scale-Model Experiments

Peter V. Nielsen

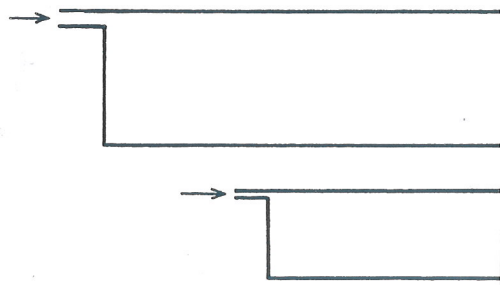

Indoor Environmental Engineering, September 1999
Department of Building Technology and Structural Engineering

ISSN 1395-8232 U9913

Lecture Notes on Scale-Model Experiments

by Peter V. Nielsen

INTRODUCTION

Large ventilated air spaces as e.g. shopping arcades, industrial buildings, atria and exhibition buildings have for a decade been built in large numbers. It is not possible to use full-scale experiments in the design of air distribution systems due to the large dimensions of such buildings. It is also difficult to use simplified design methods as for example methods based on throws of jets and penetration depths of non-isothermal jets. The reason for that is the complicated geometry which is present in many situations. Several sources that produce air movements as for example diffusers, pressure difference around buildings, cold downdraught and thermal plumes also make the use of simplified methods difficult, while Computational Fluid Dynamics and scale-model experiments are two possible methods for the determination of mass transport, contaminant transport and energy transport in large buildings.

The ventilation of a working area in an industrial environment is established by a combination of a general and a local ventilation system. The general ventilation ensures the air quality and comfort far away from the contaminants, while the local ventilation - often as exhaust hoods - ensures the contaminant transport close to the emission sources and protects the people working there. It is very important that the contaminant control system is efficient because it represents one of the first elements in a chain process that might bring the contaminant out into the room. A well-designed local ventilation system will reduce the energy consumption of the total system because it is an energy-saving method to remove the airborne pollution as close to the emission source as possible. An optimization of a local ventilation system can be made efficiently by model or full-scale experiments.

Scale-model experiments have been used to study a variety of ventilation problems as air movement in a room, air movement around a building, energy flow in a building, contaminant distribution at a operator's workplace and smoke movement in a building on fire. The theory is discussed at a general level in the references [1, 2, 3, 4, 5, 6].

GOVERNING EQUATIONS AND DIMENSIONLESS NUMBERS

Scale-model experiments are based on the similarity principles. For a physical process they can either be found from an assumption of the number of physical parameters involved (Buckinghams π-theorem) or from the governing equations of the flow. The latter is to be preferred because this method will give a sufficient amount of dimensionless numbers. Furthermore, it will connect the numbers to the physical process via the equations and give important information in cases where it is necessary to make approximations.

The governing equations for mass flow, energy flow and contaminant flow in a room will be the continuity equation, Navier Stokes equations (one in each coordinate direction), the energy equation and the mass transport equation, respectively.

The continuity equation for an incompressible flow is given by the following expression

$$\frac{\partial \hat{u}}{\partial x} + \frac{\partial \hat{v}}{\partial y} + \frac{\partial \hat{w}}{\partial z} = 0 \tag{1}$$

$\hat{u}$, $\hat{v}$ and $\hat{w}$ are the velocities in the three coordinate directions x, y, z. The symbol $\hat{}$ indicates that the variables are instantaneous values. (For example, $\hat{u}$ is the sum of a mean value u and a turbulent fluctuation u').

The Navier Stokes equation in the direction of gravity (y-direction) is given by the expression

$$\rho_o \left(\frac{\partial \hat{v}}{\partial t} + \hat{u} \frac{\partial \hat{v}}{\partial x} + \hat{v} \frac{\partial \hat{v}}{\partial y} + \hat{w} \frac{\partial \hat{v}}{\partial z} \right) = -\rho_o \beta g \left(\hat{T} - T_o \right) - \frac{\partial \hat{p}}{\partial y}$$

$$+ \mu_o \left(\frac{\partial^2 \hat{v}}{\partial x^2} + \frac{\partial^2 \hat{v}}{\partial y^2} + \frac{\partial^2 \hat{v}}{\partial z^2} \right) \tag{2}$$

$\hat{p}$, $\hat{T}$ and t are pressure, temperature and time, respectively, and T_o is a reference temperature (supply temperature). ρ_o, β, μ_o and g are density, volume expansion coefficient, viscosity and gravitational acceleration, respectively. The density and the viscosity are in principle functions of the instantaneous temperature $\hat{T}$, but except for the gravitational term the effect is ignored due to the level of temperature differences that occur in practice. $(\hat{T} - T_o)$ expresses the influence of the temperature in the gravitational term in a formulation called the Boussinesq approximation.

The energy equation is given by the expression

$$\rho_o c_p \left(\frac{\partial \hat{T}}{\partial t} + \hat{u} \frac{\partial \hat{T}}{\partial x} + \hat{v} \frac{\partial \hat{T}}{\partial y} + \hat{w} \frac{\partial \hat{T}}{\partial z} \right) = \lambda \left(\frac{\partial^2 \hat{T}}{\partial x^2} + \frac{\partial^2 \hat{T}}{\partial y^2} + \frac{\partial^2 \hat{T}}{\partial z^2} \right) \tag{3}$$

c_p and λ are specific heat and thermal conductivity.

The mass transport equation for gas in air (binary mixture) has a similar structure

$$\frac{\partial \hat{c}}{\partial t} + \hat{u} \frac{\partial \hat{c}}{\partial x} + \hat{v} \frac{\partial \hat{c}}{\partial y} + \hat{w} \frac{\partial \hat{c}}{\partial z} = D_{AB} \left(\frac{\partial^2 \hat{c}}{\partial x^2} + \frac{\partial^2 \hat{c}}{\partial y^2} + \frac{\partial^2 \hat{c}}{\partial z^2} \right) \tag{4}$$

$\hat{c}$ is the instantaneous concentration and D_{AB} is the binary mass diffusion coefficient.

Equation (4) is called an Eulerian approach because the behaviour of the species is described relative to a fixed coordinate system. The equation can also be considered to be a transport equation for particles when they are small without any influence from gravity. Flow of larger particles can be simulated by the following transport equation if the influence of gravity is introduced in the y-convection term, see reference [7, 8]

$$\frac{\partial \hat{c}}{\partial t} + \hat{u}\frac{\partial \hat{c}}{\partial x} + (v_s + \hat{v})\frac{\partial \hat{c}}{\partial y} + \hat{w}\frac{\partial \hat{c}}{\partial z} = D_{AB}\left(\frac{\partial^2 \hat{c}}{\partial x^2} + \frac{\partial^2 \hat{c}}{\partial y^2} + \frac{\partial^2 \hat{c}}{\partial z^2}\right) \tag{5}$$

v_s is the settling velocity in air. Settling velocity versus particle size is given by

$$v_s = 3 \cdot 10^{-5}\, d^2 \text{ (m/s)} \tag{6}$$

where d is the diameter in μm. The density of the particles is 1 g/cm^3 and the particles are assumed to be of spherical shape in equation (6). Simulation of concentration distribution given by equation (5) is restricted to situations where initial particle velocity and particle inertia can be ignored.

It might be necessary to describe a particle contaminant source as a distribution of particle sizes with initial velocity different from the local air velocity. A typical example of this situation is the particle distribution and particle trajectory from a grinding wheel. The particle inertia is important in this situation which makes it necessary to work with a model where the particles are treated individually through a solution of a particle motion equation. Reference [7] gives the simplified equations which govern the motion of a spherical particle (inertia equals friction and gravity forces) in a flow field. This approach is called the Lagrangian approach because the concentration changes are described relative to the moving fluid. This problem will not be considered further.

The equations (1) to (5) describe the velocity $\hat{u}$, $\hat{v}$, $\hat{w}$, the temperature distribution $\hat{T}$, the concentration distribution $\hat{c}$ (mass of gas per unit mass of mixture, particles per volume, droplet number density etc.) and pressure distribution $\hat{p}$. The variables can also be used for the calculation of air volume flow, convective air movement and contaminant transport.

It should be noted that radiant heat transfer, which can be an important part of the heat flow in a building, has not been considered.

The next step towards the similarity principles is to develop the governing equations in a non-dimensional form. The equations are normalized by first defining the dimensionless, independent variables as

$$x^* = x/h_o \qquad y^* = y/h_o \quad \text{and} \quad z^* = z/h_o \tag{7}$$

where h_o is a characteristic length of interest in the problem. A typical characteristic length in ventilation problems (general ventilation) is the height of the supply slot h_o or the square root of the supply area $\sqrt{a_o}$. The height of a hot or a cold surface ℓ can also be used as characteristic length in situations where free convection is the most important problem as for example in case of cold downdraught in an atrium at low outdoor temperatures.

The velocities

$$\hat{u}^* = \hat{u}/u_o \qquad \hat{v}^* = \hat{v}/u_o \quad \text{and} \quad \hat{w}^* = \hat{w}/u_o \tag{8}$$

are normalized by the supply velocity u_o found from

$$u_o = q_o/a_o \tag{9}$$

where q_o is the volume flow rate to the diffuser and a_o is the supply area of the diffuser.

Temperature and concentration are normalized by the following expressions

$$\hat{T}^* = \frac{\hat{T} - T_o}{T_R - T_o} \quad \text{and} \quad \hat{c}^* = \frac{\hat{c} - c_o}{c_R - c_o} \tag{10}$$

where T_o, T_R, c_o, c_R are supply temperature, return temperature, supply concentration (if any) and return concentration, respectively.

Pressure $\hat{p}$ and the independent variable time t are normalized by the following expressions

$$\hat{p}^* = \hat{p}/u_o^2 \rho_o \quad \text{and} \quad t^* = t u_o / h_o \tag{11}$$

Equations (7), (8), (10) and (11) are substituted into equations (1) to (5) and the following non-dimensionalized governing equations are obtained

$$\frac{\partial \hat{u}^*}{\partial x^*} + \frac{\partial \hat{v}^*}{\partial y^*} + \frac{\partial \hat{w}^*}{\partial z^*} = 0 \tag{12}$$

$$\frac{\partial \hat{v}^*}{\partial t^*} + \hat{u}^* \frac{\partial \hat{v}^*}{\partial x^*} + \hat{v}^* \frac{\partial \hat{v}^*}{\partial y^*} + \hat{w}^* \frac{\partial \hat{v}^*}{\partial z^*} = \frac{\beta g h_o \left(T_R - T_o\right)}{u_o^2} \hat{T}^* - \frac{\partial \hat{p}^*}{\partial y^*}$$

$$+ \frac{\mu_o}{\rho_o h_o u_o} \left(\frac{\partial^2 \hat{v}^*}{\partial x^{*2}} + \frac{\partial^2 \hat{v}^*}{\partial y^{*2}} + \frac{\partial^2 \hat{v}^*}{\partial z^{*2}} \right) \tag{13}$$

$$\frac{\partial \hat{T}^*}{\partial t^*} + \hat{u}^* \frac{\partial \hat{T}^*}{\partial x^*} + \hat{v}^* \frac{\partial \hat{T}^*}{\partial y^*} + \hat{w}^* \frac{\partial \hat{T}^*}{\partial z^*} = \frac{\lambda}{c_p \rho_o h_o u_o} \left(\frac{\partial^2 \hat{T}^*}{\partial x^{*2}} + \frac{\partial^2 \hat{T}^*}{\partial y^{*2}} + \frac{\partial^2 \hat{T}^*}{\partial z^{*2}} \right) \tag{14}$$

$$\frac{\partial \hat{c}^*}{\partial t^*} + \hat{u}^* \frac{\partial \hat{c}^*}{\partial x^*} + \hat{v}^* \frac{\partial \hat{c}^*}{\partial y^*} + \hat{w}^* \frac{\partial \hat{c}^*}{\partial z^*} = \frac{D_{AB}}{h_o u_o} \left(\frac{\partial^2 \hat{c}^*}{\partial x^{*2}} + \frac{\partial^2 \hat{c}^*}{\partial y^{*2}} + \frac{\partial^2 \hat{c}^*}{\partial z^{*2}} \right) \tag{15}$$

$$\frac{\partial \hat{c}^*}{\partial t^*} + \hat{u}^* \frac{\partial \hat{c}^*}{\partial x^*} + \left(\frac{v_s}{u_o} + \hat{v}^* \right) \frac{\partial \hat{c}^*}{\partial y^*} + \hat{w}^* \frac{\partial \hat{c}^*}{\partial z^*} = \frac{D_{AB}}{h_o u_o} \left(\frac{\partial^2 \hat{c}^*}{\partial x^{*2}} + \frac{\partial^2 \hat{c}^*}{\partial y^{*2}} + \frac{\partial^2 \hat{c}^*}{\partial z^{*2}} \right) \tag{16}$$

It is observed that the following dimensionless numbers appear in the equations

$$Ar = \frac{\beta g h_o \left(T_R - T_o\right)}{u_o^2} \tag{17}$$

$$Re = \frac{\rho_o h_o u_o}{\mu_o} \tag{18}$$

$$Pr = \frac{\mu_o c_p}{\lambda} \tag{19}$$

$$Sc = \frac{\mu_o}{\rho_o D_{AB}} \tag{20}$$

$$v_s^* = \frac{v_s}{u_o} \tag{21}$$

Ar, Re, Pr, Sc and v_s^* are called Archimedes number, Reynolds number, Prandtl number, Schmidt number and the settling velocity ratio, respectively.

The Archimedes number may be considered as a ratio of thermal buoyancy force to inertial force, while the Reynolds number may be looked upon as a ratio of inertial force to viscous force. The Reynolds number can also be considered as the ratio of turbulent diffusion to laminar diffusion. The Prandtl number is the ratio of momentum diffusivity to thermal diffusivity, while the Schmidt number is the ratio of momentum diffusivity to mass diffusivity.

Ar and $1/Re$ appear in the Navier Stokes equations (equation (13)) and $1/(RePr)$ in the energy equation (equation (14)). $1/(ReSc)$ appears in the transport equations for contaminants (equations (15) and (16)) and the settling velocity ratio v_s^* appears in the contaminant transport equation for large particles (equation (16)).

The dimensionless numbers are important elements in the performance of model experiments and they are determined by the normalizing procedure of the independent variables. If, for example, free convection is considered in a room without ventilation it is not possible to normalize the velocities by a supply velocity u_o. The normalized velocity can be defined by $\hat{u}^* = \hat{u}\ell\rho_o/\mu_o$ where ℓ is the height of a cold or a hot surface. The Grashof number Gr will then appear in the buoyancy term in the Navier Stokes equation

$$Gr = \frac{\beta g \rho_o^2 \ell^3 \left(T_R - T_o\right)}{\mu_o^2} \tag{22}$$

The Grashof number can be expressed as

$$Gr = ArRe^2 \tag{23}$$

SIMILARITY PRINCIPLES AND CONDITIONS FOR MODEL EXPERIMENTS

The general conditions for scale-model experiments with flow in a room are

1) identical dimensionless sets of boundary conditions, including geometry, in room and in model,

2) identical dimensionless numbers, equations (17) to (21), in the governing equations for the flow in the room and in the model,

3) the constants ρ_o, β, μ_o, ... in the governing equations (equations (1) to (5)) should only have a small variation within the applied temperature and velocity levels.

The requirements of identical dimensionless boundary conditions are met when the model is geometrically similar to full scale in all details that are important for the volume flow, the energy flow and the contaminant flow, see figure 1. The dimensionless supply profile from the diffuser in an experiment with general ventilation given by

$$\hat{u}^*,\ \hat{v}^*,\ \hat{w}^* = f(x, y, z, t) \tag{24}$$

must thus be identical for both room and model. This can be obtained by using a diffuser in the model which is geometrically similar to the expected diffuser in the room, but it is an expensive solution because it is difficult to reproduce all the details in the diffuser when the model for example is one tenth of full scale. The problem can be simplified if it is possible to replace the diffuser by a simple opening which is able to generate a similar flow in the model. The problem is somewhat similar to the use of the Inlet-Box Method or the Prescribed Velocity Method in Computational Fluid Dynamics.

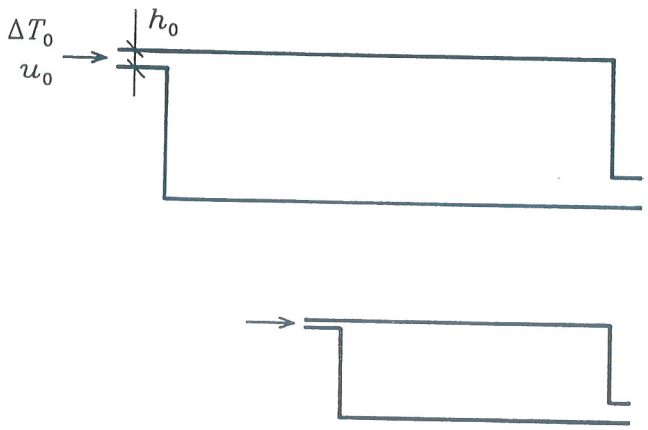

Figure 1. Full-scale room with slot inlet and a similar scale model.

Figure 2 shows an example of the use of a simplified supply opening in the model. The diffuser in the room is mounted on the end wall and it supplies the air through a row of small openings at an angle of 45 degrees towards the ceiling. This diffuser is simulated in a model experiment by a nozzle which supplies a jet in the same direction towards the ceiling, see figure 2. Figure 3 shows the velocity decay of centre line velocity u_x versus distance x in the two cases. The agreement between the velocity decay from the diffuser and the decay in the model seems to be fair.

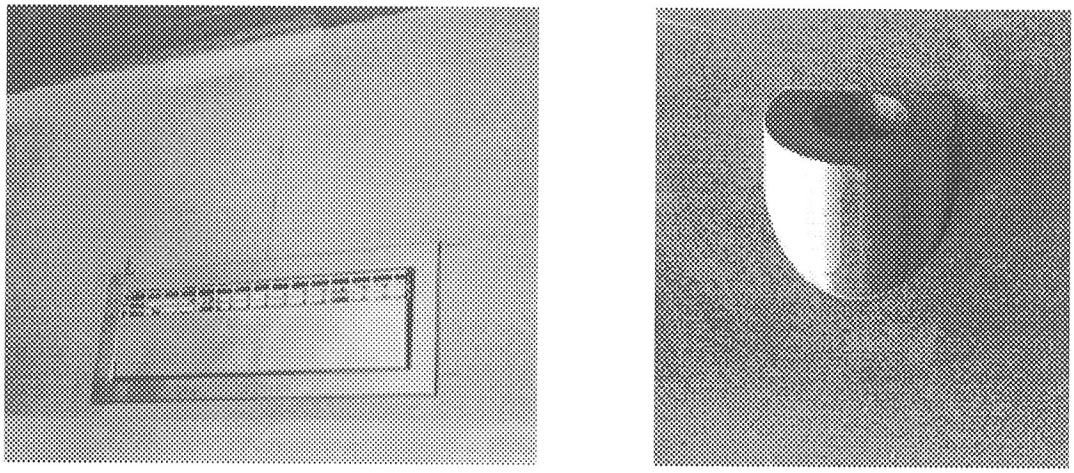

Figure 2. Wall-mounted diffuser in a full-scale test room and a nozzle in a model room.

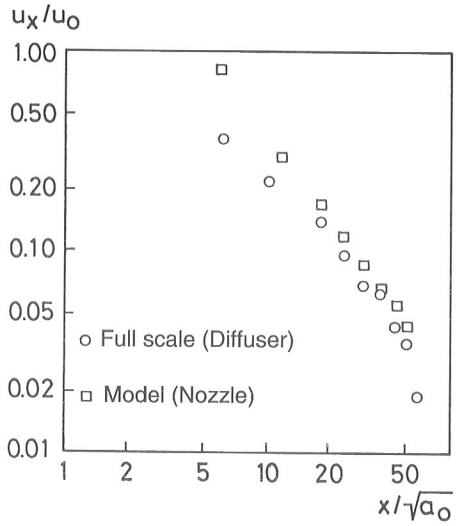

Figure 3. Velocity decay in a wall jet along the ceiling in a room and in a model.

It is difficult to obtain the correct temperature boundary conditions in the model. Radiation between surfaces in a room and conduction through the surfaces are important for the level of the surface temperature $T_s\ (x, y, z)$. It is difficult to establish similar principles based on radiation and conduction. A practical method is to estimate the influence of radiation and conduction and include this level in the boundary values of the model. In this way it is possible to obtain an identical dimensionless temperature distribution $T_s^*\ (x, y, z)$ in full scale and in model.

The conditions for model experiments can be explained in the following way. The governing equations are made non-dimensional in full scale and in the reduced scale used in the model experiments. For example, the velocities in the room equations are divided by the diffuser velocity in the room, and the velocities in the model equations are divided by the supply velocity in the model in order to normalize all velocities. The two sets of equations are identical and they describe the same solution provided that the requirements 1), 2) and 3) mentioned at the beginning of this section have been met.

It is difficult to carry out a model experiment on a reduced scale if all the dimensionless numbers must be kept constant. If, for example, the scale is reduced by a factor of 10, then the velocity also has to be

increased by a factor of 10 due to the Reynolds number which will give an increase in the temperature difference by a factor of 1000 in order to keep the Archimedes number. The Prandtl number is, on the other hand, unchanged when air is used as the fluid in the model experiments. The problem with the temperature level can be slightly reduced when water is used as fluid in the model experiments and, as shown in the next section, the problem can also be reduced when the flow is a fully developed turbulent flow.

It is only possible to obtain similar solutions in situations where the governing equations (equations (1) to (5)) are identical in full scale and in model. This requirement will be met in situations where the same dimensionless numbers are used in full scale and in model and when the constants $\rho_o, \beta, \mu_o, \ldots$ only have a small variation within the applied temperature and velocity level. A practical problem when water is used as fluid in the model is the variation of β which is very different in air and in water, see figure 4. Therefore, it is necessary to restrict the temperature differences used in model experiments based on water.

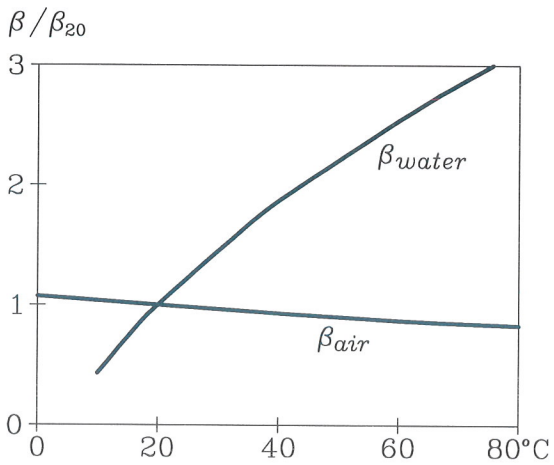

Figure 4. Relative change in the volume expansion coefficient for air and water.

MODEL EXPERIMENTS IN THE CASE OF FULLY DEVELOPED TURBULENT FLOW

The problems that arise when experiments are carried out in a greatly reduced scale can be overcome if the Reynolds number is high and the flow pattern is governed mainly by fully developed turbulence. It is possible to ignore the Reynolds number, the Schmidt number and the Prandtl number because the structure of the turbulence and the flow pattern at a sufficiently high level of velocity will be similar at different supply velocities and therefore independent of the Reynolds number. The transport of thermal energy and mass by turbulent eddies will likewise dominate the molecular diffusion and will therefore also be independent of the Prandtl number and the Schmidt number.

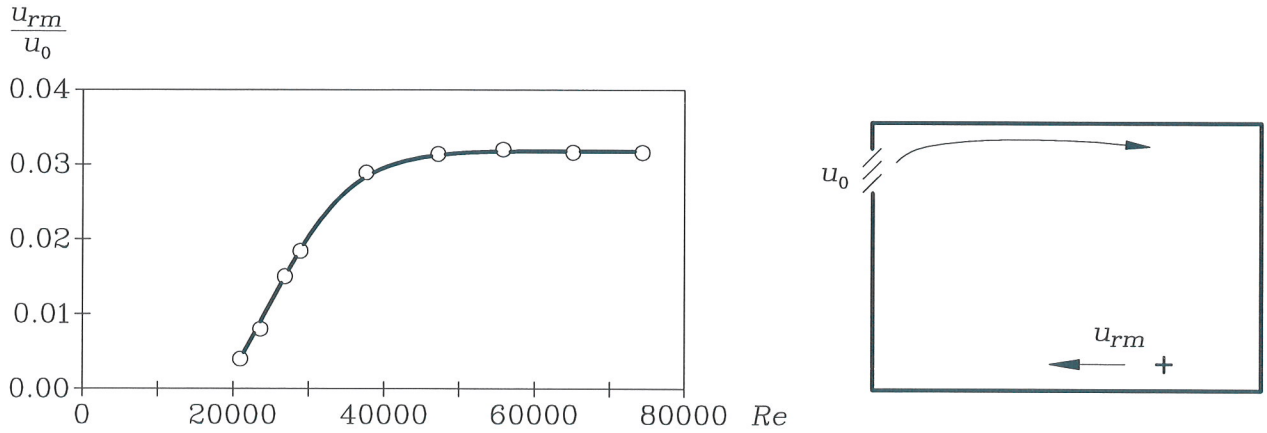

Figure 5. Normalized velocity versus Reynolds number in a ventilated room, see reference [4].

Figure 5 shows as an example how the dimensionless maximum velocity in a room u_{rm}/u_o is constant at different supply velocities u_o for Reynolds numbers larger than 45000. This value is called the critical Reynolds number Re_c. A model experiment with isothermal flow in the room as in figure 5 can therefore be carried out at any Reynolds number larger than Re_c if the full-scale flow has a Reynolds number which is larger than Re_c. It is also obvious that the Reynolds number must have the same value in full scale and in model for Reynolds numbers smaller than Re_c.

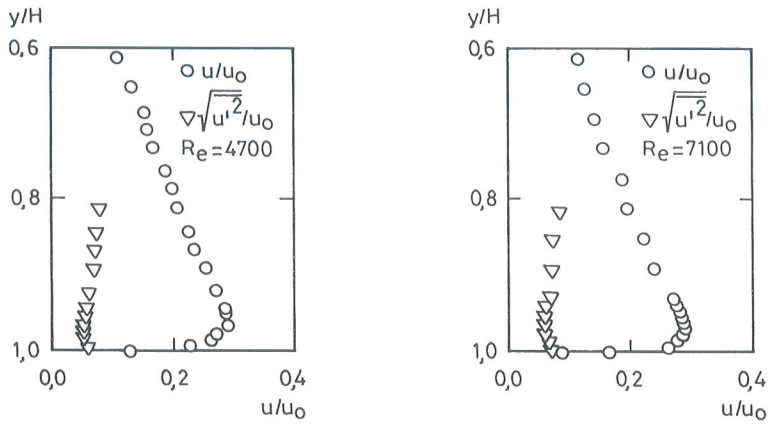

Figure 6. Velocity distribution and turbulence intensity in the occupied zone of a room at two different Reynolds numbers. H is the height of the room.

The similarity of velocity and of turbulence intensity is documented in figure 6. The figure shows a vertical dimensionless velocity profile and a turbulence intensity profile measured by isothermal model experiments at two different Reynolds numbers, reference [9].

It is necessary to study the possibility of Reynolds number independence in full scale and in model as part of a complete model experiment.

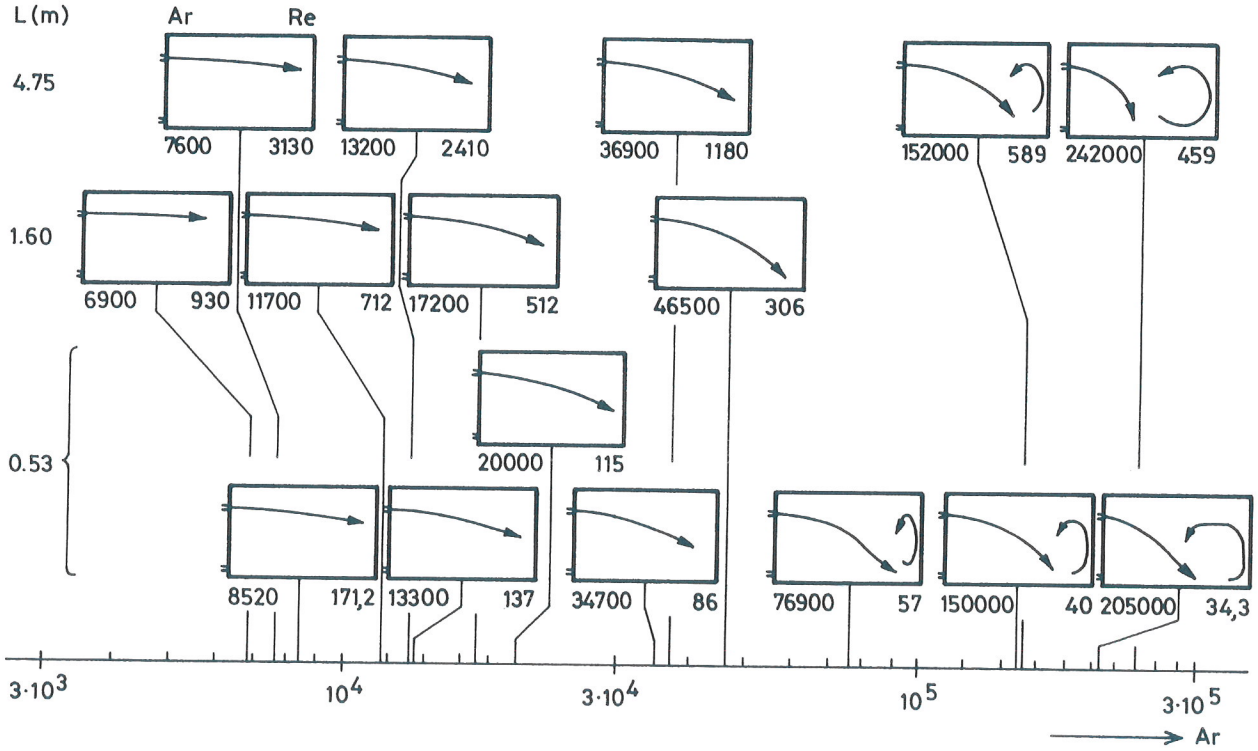

Figure 7. Model experiments with non-isothermal flow in three different models with ceiling heating.

Fully developed non-isothermal flow may also be similar at different Reynolds numbers, Prandtl numbers and Schmidt numbers. The Archimedes number will, on the other hand, always be an important parameter. Figure 7 shows a number of model experiments performed in three geometrically identical models with the heights 0.53 m, 1.60 m and 4.75 m, see reference [10]. Sixteen experiments carried out in the rooms at different Archimedes numbers and Reynolds numbers show that the general flow pattern (jet trajectory of a cold jet from a circular opening in the wall) is a function of Archimedes number but independent of the Reynolds number. (The characteristic length and velocity in figure 7 are defined as $\ell = 4\,WH/(2\,W + 2\,H)$ and $u = q_o/WH$ where W is the width of the room and H is the height of the room).

The neglect of a low turbulence effect and a laminar flow is not justified in regions close to solid surfaces where the turbulent velocity fluctuations must tend to zero. In experiments where the correct level of heat transfer and mass transfer through the boundary layer is important it is necessary to take all dimensionless numbers involved into full consideration. It is possible to draw a parallel to the situation in Computational Fluid Dynamics where a k–ε turbulence model describes the main flow clear of surfaces as a fully developed turbulent flow used together with wall functions which take the low turbulent effect and laminar flow close to surfaces into consideration.

Model experiments where free convection is the important part of the flow are expressed by the Grashof number instead of the Archimedes number, see equation (22). The general conditions for scale- model experiments are the use of the identical Grashof number Gr, the Prandtl number Pr and the Schmidt number Sc in the governing equations for the room and in the model.

A practical approach is to simulate cold or hot surfaces with replacement jets which match the air flow in the model to the flow in the full-size room. This method is described by Nevrala and Probert, see reference [11].

MODEL EXPERIMENTS IN CONNECTION WITH LOCAL VENTILATION IN THE INDUSTRIAL ENVIRONMENT

Experiments on the scale of 1 to 1 are often used to study the local ventilation around an operator's workplace. Tracer gas is used to simulate the contaminant transport and a high concentration level of the model tracer gas makes it possible to work with a convenient level of concentration for the measurements. Figure 8 shows an enclosure with an emission source S and a laboratory set-up with a model source S_t. The dimensionless concentration c/c_R is identical with c_t/c_{Rt} in the laboratory model if the Archimedes numbers are identical in full scale and in model, and if the Reynolds numbers in both cases are identical or above the critical value for a fully turbulent flow.

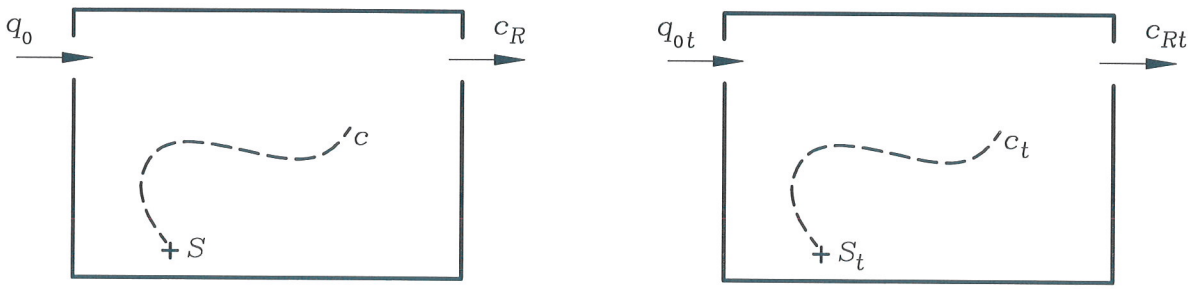

Figure 8. Enclosure with a contaminant source S and a laboratory model with a model source S_t.

The concentration at a given position close to an emission source can be calculated from

$$c = c_t \frac{c_R}{c_{Rt}} \tag{25}$$

where c_t, c_{Rt} and c_R are tracer gas concentration at the corresponding position in the laboratory model, tracer gas concentration in the reference point in the laboratory model (return opening) and contaminant concentration in the reference point, respectively.

The emission source S can be found from

$$S = S_t \frac{c}{c_t} \frac{q_o}{q_{ot}} \tag{26}$$

where q_o is the volume flow around the local ventilation and q_{ot} is the volume flow around the model.

LABORATORY EXPERIMENTS WITH GENERAL AND LOCAL VENTILATION

This section shows some examples of the use of model experiments. The examples cover the range from natural ventilation of buildings, comfort ventilation of an exhibition hall to local ventilation in industrial areas.

The Danish Pavilion in Seville

The Danish Pavilion at the EXPO '92 World Exhibition is shown in figure 9. It has two main elements:

a steel framed structure, facing west, with a floor area of 45.0 m × 2.5 m and a height of 24 m, and a fibre glass construction, facing east, which leans against the steel structure. The large room formed between the fibre glass surface and the steel building is enclosed by glass walls to the north and to the south. This room is the exhibition hall and it was visited by more than 800,000 people during EXPO '92.

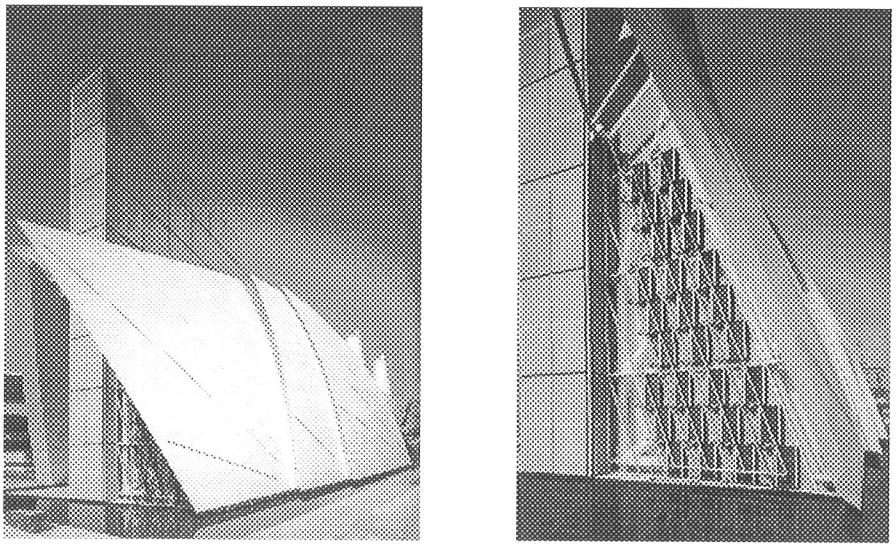

Figure 9. The Danish Pavilion at the World Exposition EXPO '92 in Seville and the cooling elements in the south gable.

The occupied zone design load of the exhibition hall is 48 kW corresponding to 300 persons in the pavilion. The equipment for slides and video will generate another 130 kW which is expected to move upwards in convective flows causing a high temperature in the upper part of the pavilion.

The ventilation system is based on an extract fan in the north top of the exhibition hall (smoke ventilation) and on exposed cooling elements in the south gable, see figure 9. Air is drawn through the cooling elements where it cools and falls to the floor. It is difficult to give an estimate of the downdraught from the 12 m high diffuser in the gable and therefore it was decided to carry out scale-model experiments and Computational Fluid Dynamics predictions of the flow.

The model experiments were carried out in a model on the scale of 1 to 10. Experience with measurements on flow from wall-mounted diffusers for displacement ventilation indicates that it is possible to ignore the level of the Reynolds number at the given dimensions which will enable reasonable temperature differences in the model experiments.

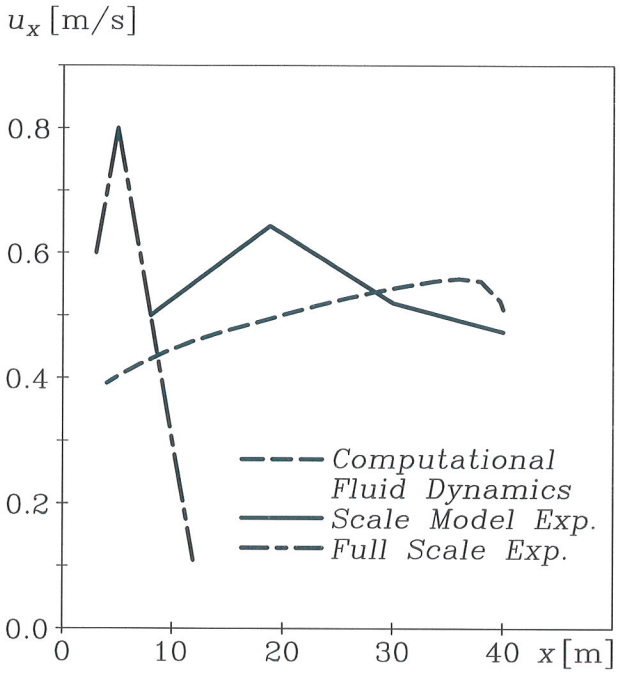

Figure 10. Velocity distribution in the restaurant and exhibition hall of the Danish Pavilion.

Figure 10 shows the velocity distribution down through the full length of the exhibition hall. It is quite obvious that the flow is a stratified flow with the highest velocity in the occupied zone. Smoke measurements show that the cold air from the cooling device accelerates down into the occupied zone, due to gravity, and moves horizontally as a stratified flow along the floor in the restaurant and exhibition section.

Measurements show that the velocity has a fairly constant level in the occupied zone even far downstream from the wall with the cooling device. The flow is plane and it is a general experience that the velocity in a plane stratified flow is constant and independent of the distance from the inlet device. Prediction of the flow by Computational Fluid Dynamics shows a similar velocity level in the hall, see reference [12]. The full-scale measurements shown in figure 10 indicate a very low velocity in most of the hall. The reason for that was the practical difficulties in obtaining a correct load during the full-scale experiment .

School building

Experiments with natural ventilation of large constructions as e.g. shopping arcades and atria necessitate a set of boundary conditions outside the openings in the building because the pressure distribution (and flow) around a building are an important part of the problem.

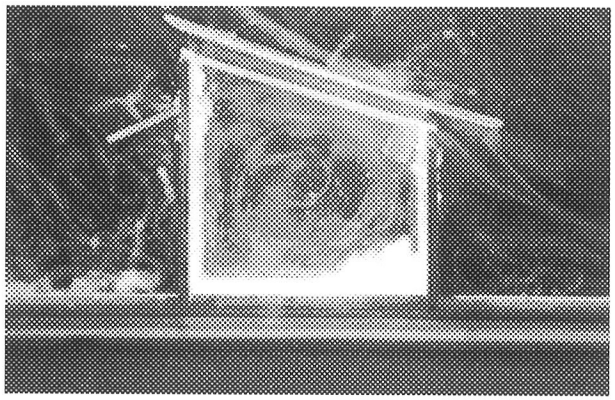

Figure 11. Scale-model experiment with natural ventilation of a school building.

The experiments have to be carried out in an environmental wind tunnel, se references [3] and [13]. A roughness on the surface in such a wind tunnel generates a typically vertical profile, and the whole building and the neighbouring buildings are exposed to the flow. Figure 11 illustrates an experiment. The flow around a model of a school building in Tanzania is shown by the stream lines of lightweight particles in the air. It is possible to study the flow in the double ceiling, the flow through the window openings and the recirculating flow in the class room.

Filling machine

The contaminant source considered in this section is a filling machine for painting. Figure 12A shows the machine with a filling tube (to the left in the figure) and equipment for closing of the cans (to the right in the figure). The machine was originally delivered without exhaust equipment but an exhaust opening has been mounted behind the filling tube. Measurements at the operator's workplace show an exhaust flow rate of 180 m^3/h and an acceptable air quality in the operator's breathing zone.

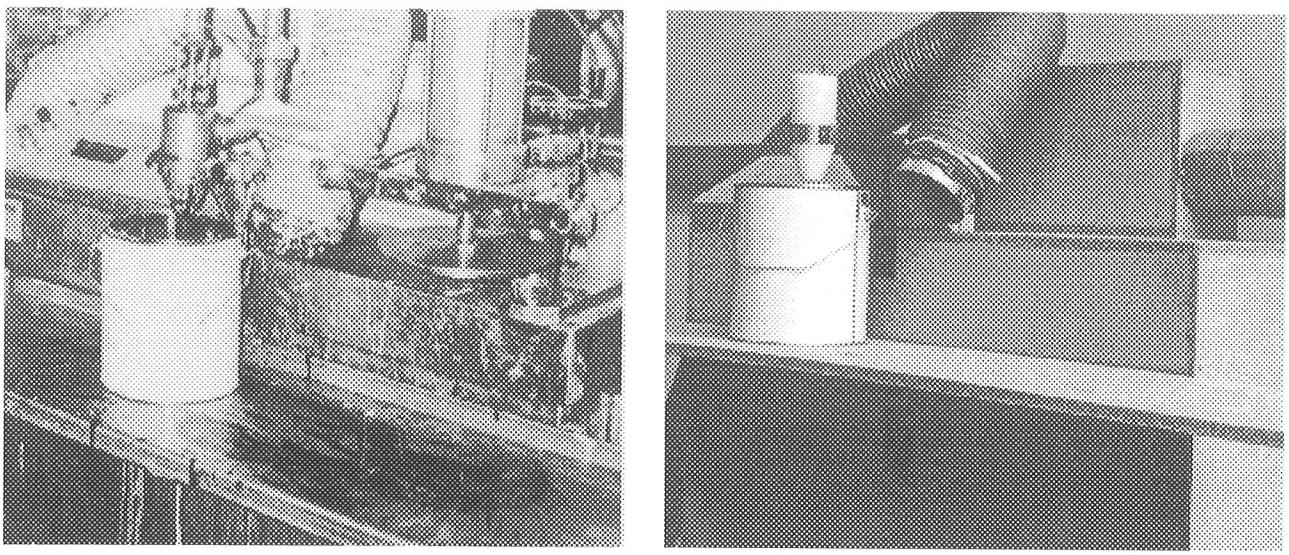

A B

Figure 12. A: filling machine from the paint industry and B: full-scale model of the machine.

Figure 12B shows a model of the machine on the scale of 1 to 1. Many details and surfaces are made in the correct size and location to achieve a good reproduction of the actual capturing zone. The capture efficiency α is used for the evaluation of the system and it is defined as the ratio between the flow rate of the contaminant S_E directly captured from the process and the total flow rate of the contaminant S released from the process

$$\alpha = \frac{S_E}{S} \tag{27}$$

Figure 13 shows the capture efficiency as a function of the exhaust flow rate q_E both with the emission source at the filling position and with the emission source at the closing position. The last position shows the lowest values in capture efficiency due to the distance to the exhaust opening. The shaded area in the figure corresponds to the position between the filling and the closing of the cans.

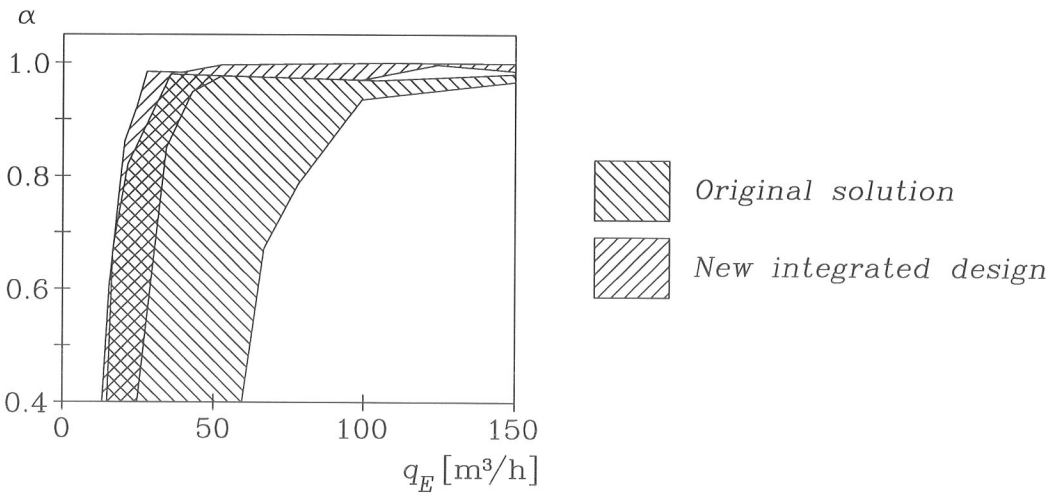

Figure 13. Capture efficiency versus flow rate for the original solution and for the new integrated design.

The exhaust air represents a high energy consumption and therefore it is important to have a design with a high capture efficiency at low flow rates. Figure 14 shows a new design of the exhaust opening where parts of the machine are integrated into the opening and in this way act as flanges for the flow. It is shown in figure 13 that this solution makes it possible to decrease the flow substantially (by 65%) and still keep the high capture efficiency, see reference [14].

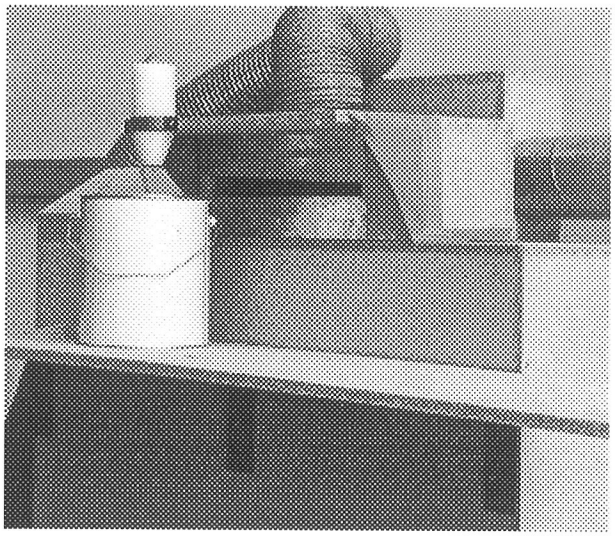

Figure 14. New design of an exhaust opening integrated into the can filling machine.

Generally it must be concluded that the exhaust openings should be an integrated part of the machine or the equipment to obtain an optimal solution.

Film developing machine

Figure 15 shows a film developing machine and the corresponding model for laboratory experiments on the scale of 1 to 1. The machine consists of two sections, a developing section in the lower part and an air drying section in the upper part. The new-developed films leave the air drying section through the opening shown in the upper part of the figure. Air is supplied to the drying section from ventilators and is blown out into the surroundings through the opening for the films and, consequently, it causes low air quality in the room. There is also an additional problem because the operator of the developing machine will be highly exposed when he stands in front of the machine and changes the films.

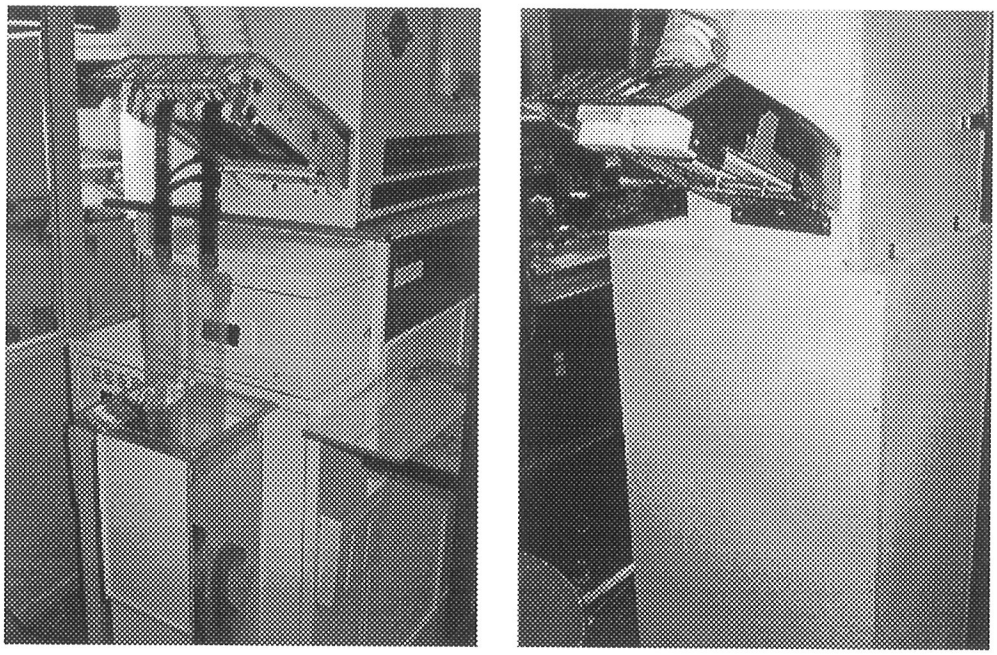

Figure 15. Film developing machine and a laboratory model.

The initial solution of this problem was to install an exhaust channel on the opening for the films, see figure 15. Laboratory experiments show that the principle is inexpedient and that it is only possible to obtain a capture efficiency of 70% at a flow rate of 100 m^3/h.

The experiments show that it is impossible to make a simple design of the opening which can improve the air quality in the room. A proper solution should have been chosen in the design phase of the machine. It would for example be obvious to reverse the direction of the air flow and extract the air from the room through the machine.

Vortex exhaust

The vortex exhaust has a geometry which generates a rotating flow behind the opening. It is suitable for installation in a narrow space and it is traditionally used with hand-held equipment which generates jets of air and particles. This type of exhaust opening is also called a tornado exhaust or a cyclone exhaust.

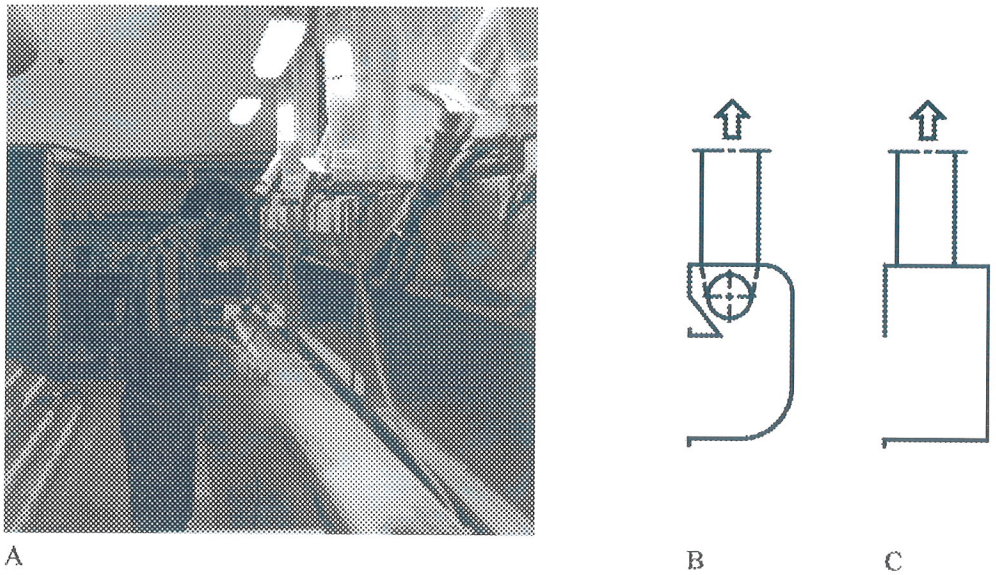

Figure 16. A: vortex exhaust at a concrete element factory, B: laboratory model of the vortex exhaust and C: simplified model of the exhaust.

Figure 16A shows an exhaust opening used for capture of concrete dust from a hand-held grinding machine. The figures 16B and 16C show two laboratory models. Both models are made on the scale of 1 to 2. The first model (figure 16B) is identical with the real opening, while the other model has a simplified geometry.

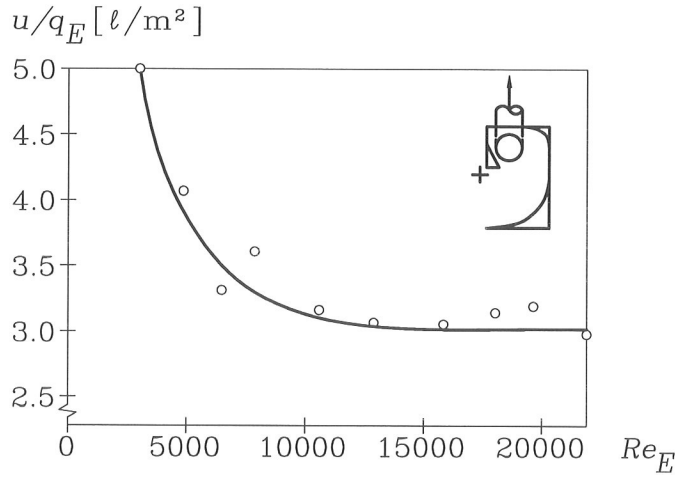

Figure 17. Normalized velocity versus Reynolds number for a vortex exhaust. The location of the measuring point is indicated in the figure.

A reduced scale of the model requires an increased velocity level in the experiments to obtain the correct Reynolds number if $Re < Re_c$, but the experiment can be carried out at any velocity if $Re > Re_c$. The influence of the turbulence level is shown in figure 17. A velocity u is measured at a location in front of the opening and it is divided by the exhaust flow rate q_E in order to obtain a normalized velocity. The figure shows that the normalized velocity is constant for Reynolds numbers larger than 10,000, which means that the flow has a fully developed turbulent structure in the vortex exhaust at that velocity level. The flow may be described as a potential flow with a normalized velocity independent of the exhaust flow rate at large distances from the exhaust opening - and far away from surfaces.

Comparisons between measurements on the two geometries, figures 16B and C, show that a rotating flow will be generated in both cases. The T-shaped exhaust opening in the middle of the rotating flow in the original design is not the only element which generates the vortex, the asymmetry is also important as a source of vortex flow. The T-connection will smooth the capture velocity in the horizontal direction compared with the velocity distribution obtained in the simplified design.

It is important that the vortex exhaust has a high capture efficiency in connection with blasts from high-pressure air cleaning equipment. The geometry is designed to capture jets from different directions and experiments with two versions (figures 16B and C) indicate that both versions have high capture efficiency of concentrated jets.

The T-connection in the original vortex exhaust will increase the pressure loss and increase the consumption of energy. Measurements of the pressure difference in the two versions show a seven times higher pressure difference in the original version (figure 16B) compared with the pressure difference in the simplified version (figure 16C). This fact is very important in connection with the selection of a given solution.

THE USE OF SIMILARITY PRINCIPLES IN THE PLANNING OF EXPERIMENTS

It is useful to take the similarity principles and the dimensionless numbers into consideration when experiments are planned. Experiments may involve different levels of velocities and temperature differences. It is important to select values which give a large variation of the Archimedes number (17) to obtain a high possibility of large physical effects in the measurements.

The assumption of a self-similar flow (Reynolds number independent flow) simplifies full-scale experiments and is also a useful tool in the formulation of a measuring procedures. This section will show two examples of self-similar flow where the Archimedes number is the only important parameter.

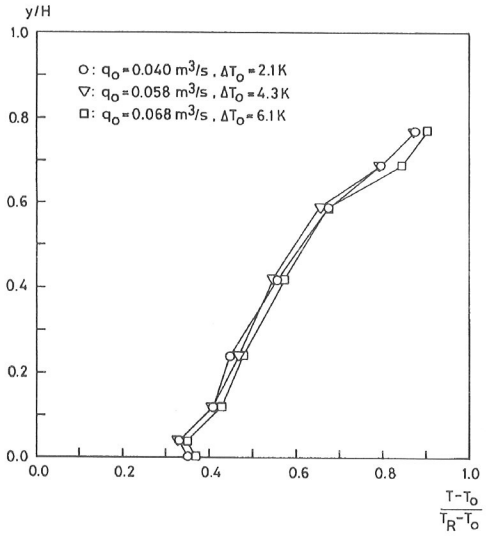

Figure 18. Vertical temperature profile in the room for three different experiments with identical Archimedes number, reference [15].

Figure 18 shows the results of three experiments with similar Archimedes number and different Reynolds numbers. The figure shows vertical temperature profiles in a room ventilated by displacement ventilation. The dimensionless profiles are similar within the flow rates shown in the figure, although the profile may involve areas with a low turbulence level in the middle of the room. A test of this type could indicate that further experiments can be performed independently of the Reynolds numbers.

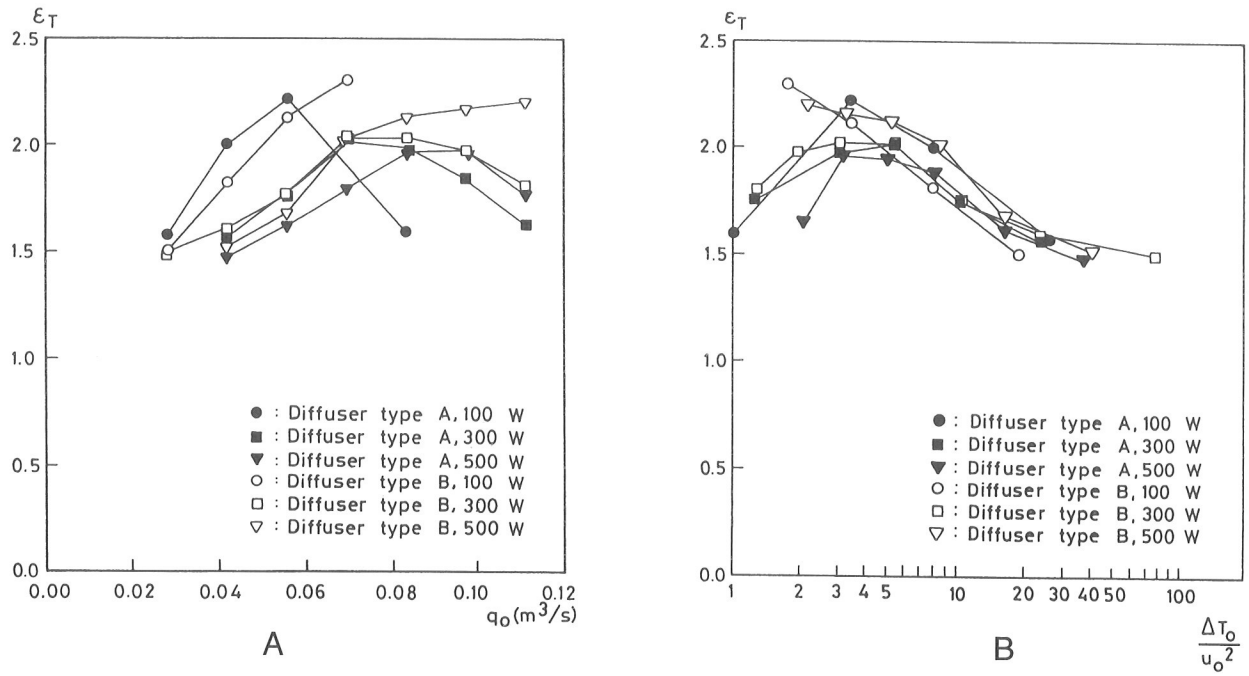

Figure 19. Temperature effectiveness versus air flow rate q_o and Archimedes number $\Delta T_o/u_o^2$, reference [15].

Figure 19 shows another example of the use of similarity principles in experiments. The temperature effectiveness ε_T is measured in a room ventilated by displacement ventilation. The measurements are made at different flow rates q_o to the room, at different loads (from 100 W to 500 W) and by two different wall-mounted diffusers. Figure 19A shows ε_T values between 1.5 and 2.3, however, it is difficult to reach other conclusions from this figure as for example the importance of the two different diffusers.

Figure 19B shows the measurements given as a function of the Archimedes number $Ar \sim \Delta T_o / u_o^2$. This figure is more informative than figure 19A. The figure shows that the temperature effectiveness ε_T is a function of the Archimedes number. An identical level of ε_T for the two diffusers A and B at the same Archimedes number implies that the temperature effectiveness is rather independent of the diffuser design and the local induction close to the diffuser. The effectiveness is probably more dependent on other parameters which are constant in the experiments, such as heat source and heat source location.

REFERENCES

1. Mierzwinski, S., Scale Model Experiments, Chapter in Ventilation of Large Spaces in Buildings, Editors: P. Heiselberg, S. Murakami and C.-A. Roulet, IEA, Energy Conservation in Buildings and Community Systems, Annex 26, ISSN 1395-7953 R9803, Aalborg University, Aalborg, Denmark, 1998.

2. Awbi, H.B., Ventilation of Buildings, Chapman and Hall, London, 1991.

3. Etheridge, D. and Sandberg, M., Building Ventilation, Theory and Measurement, John Wiley & Sons, Chichester, 1996.

4. Nielsen, P.V., Model Experiments for the Determination of Airflow in Large Spaces, Proc. of the 6th International Conference on Indoor Air Quality and Climate, Indoor Air '93, Helsinki, Finland, 1993.

5. Nielsen, P.V., Design of Local Ventilation by Full-Scale and Scale Modelling Techniques, Proceedings of the 5th International Symposium on Ventilation for Contaminant Control, Ventilation '97, Ottawa, Canada, Vol. 1, pp. 47-57, September 14-17,1997.

6. Kato, S., Murakami, S., Kong, C.N. and Nakagawa, H., Model Experiment on Indoor Climate and Space Air Distribution in Large-Scale Room, Proc. of the International Symposium on Scale Modeling, The Japan Society of Mechanical Engineers, 1988.

7. Nielsen, P.V., Prospects for Computational Fluid Dynamics in Room Air Contaminant Control, Proc. of the 4th International Symposium on Ventilation for Contaminant Control, Ventilation '94, Stockholm, 1994.

8. Murakami, S., Kato, S., Nagano, S. and Tanaka, Y., Diffusion Characteristics of Airborne Particles with Gravitational Settling in a Convective-Dominant Indoor Flow Field. ASHRAE Transactions, V. 98, Pt. 1 (1992) 82-97.

9. Nielsen, P.V., Flow in Air Conditioned Rooms, Ph.D. Thesis, Technical University of Denmark, 1974.

10. Müllejans, H., Über die Ähnlichkeit der nicht-isothermen Strömung und den Wärmeübergang in Räumen mit Strahllüftung, Ph.D. Thesis,T. H. Aachen, 1963.

11. Nevrala, D.J., Probert, S.D., Modelling Convective Currents in Rooms by Means of Wall Jets, Building Services Engineering Research & Technology, Vol. 2, No. 1, 1981.

12. Nielsen, P.V., Airflow in a World Exposition Pavilion Studied by Scale-Model Experiments and Computational Fluid Dynamics, ASHRAE Transactions, Vol. 101, Part 2, pp. 1118-1126, 1995.

13. Lawson, T.V., Wind Effect on Buildings, Applied Science Publishers, London, 1980.

14. Nielsen, P.V., Madsen, U. and Tveit, D.J., Experiments on an Exhaust Hood for the Paint Industry. Ventilation '91, Cincinnati, 1991.

15. Nielsen, P.V., Displacement Ventilation in a Room with Low-Level Diffusers, Kälte-Klima-Tagung, Deutscher Kälte- und Klimatechnischer Verein e.V., 1988.

Lecture N

ISSN 1395-8232 U9913
Dept. of Building Technology and Structural Engineering
Aalborg University, September 1999
Sohngaardsholmsvej 57, DK-9000 Aalborg, Denmark
Phone: +45 9635 8080 Fax: +45 9814 8243
http://iee.civil.auc.dk